J. Fluid Mech. (1989), *vol.* 201, *pp.* 147–166
Printed in Great Britain

Double-diffusive convection in a porous medium

By B. T. MURRAY† AND C. F. CHEN‡

†Department of Mechanical Engineering and Mechanics, Lehigh University, Bethlehem, PA 18015, USA

‡Department of Aerospace and Mechanical Engineering, University of Arizona, Tucson, AZ 85721, USA

(Received 7 August 1987 and in revised form 14 September 1988)

An experimental study has been carried out to examine double-diffusive convection in a porous medium. The experiments were performed in a horizontal layer of porous medium consisting of 3 mm diameter glass beads contained in a box 24 cm × 12 cm × 4 cm high. The top and bottom walls were made of brass and were kept at different constant temperatures by separate baths, with the bottom temperature higher than that of the top. The onset of convection was detected by a heat flux sensor and by the temperature distribution in the porous medium. When the porous medium was saturated with distilled water, the onset of convection was marked by a change in slope of the heat flux curve. The temperature distribution in the longitudinal direction in the middle of the layer indicated a convection pattern consisting of two-dimensional rolls with axes parallel to the short side. This pattern was confirmed by flow visualization. When the porous medium was saturated with salinity gradients of 0.15% cm^{-1} and 0.225% cm^{-1}, the onset of convection was marked by a dramatic increase in heat flux at the critical ΔT, and the convection pattern was three-dimensional. When the temperature difference was reduced from supercritical to subcritical values, the heat flux curve established a hysteresis loop. Results from linear stability theory, taking into account effects of temperature-dependent viscosity, volumetric expansion coefficients, and a nonlinear basic state salinity profile, are discussed.

1. Introduction

Convective fluid motion in porous media has been the subject of intensive study because of its importance in the prediction of ground-water movement in aquifers, in the energy extraction process from geothermal reservoirs, in assessing the effectiveness of fibrous insulations, and in nuclear engineering. Interest in research in this field has prompted the appearance of two excellent review articles, by Combarnous & Bories (1975) and Cheng (1978). It is known that, in many areas of the world, geothermal reservoirs and aquifers are saturated with fluids of relatively high salinity, such as those found in the Imperial Valley where salinity as high as 25% has been reported (Cheng 1978), in the Floridian aquifer (Kohout 1965), and in Israel near Lake Kinnert (Rubin 1973). With the simultaneous presence of salt and temperature gradients, the transport process can be drastically modified, from that due to temperature gradients alone, by double-diffusive effects. To understand such convective phenomena, we have carried out an experimental study on the effect of

† Now at the National Bureau of Standards, Gaithersburg, Maryland.

a stable salinity gradient on the onset of convection in a porous layer when heated from below.

It is known that in viscous fluids, when a salinity gradient is being heated from below, hysteresis in the transport of heat and salt has been observed. Krishnamurti & Howard (1985) studied double-diffusive convection in a fluid layer experimentally using heat and NaCl as the diffusing components. They measured both the heat and salt transfer across the layer. They found that at onset the heat and salt transfer increased to several times the diffusion values and that, when the temperature difference across the layer was reduced, the heat and solute transfer exhibited a marked hysteresis. It is of interest to investigate if such hysteresis phenomenon occurs in a porous medium in which there is increased damping.

Caldwell (1974) used the Soret effect to set up the initial salinity gradient in an experimental study for the fluid case. Once the stabilizing salinity gradient was established, Soret transport did not affect the dynamics of the double-diffusive mechanism. Caldwell detected the oscillatory behaviour predicted by linear theory initially, but found steady motion away from onset. He also observed hysteresis, with steady convection being maintained below the onset temperature difference as the destabilizing influence of the heat input was reduced.

The onset of convection in a horizontal layer saturated with a fluid of uniform concentration was considered by Horton & Rogers (1945) and by Lapwood (1948) using linear stability theory. For a layer confined between rigid and perfectly conducting walls, they predicted a critical Rayleigh number of $4\pi^2$ and a critical wavelength of $2d$, where d is the thickness of the layer. In an effort to confirm this theoretical result by experiments, both Elder (1967) and Katto & Masuoka (1967) suggested independently that the thermal Rayleigh number should be defined by an equivalent thermal diffusivity κ^*:

$$R_T = \frac{g\alpha \Delta T K d}{\nu \kappa^*}, \tag{1}$$

where g is the gravitational acceleration, α is the volumetric expansion coefficient $-\rho^{-1}\partial\rho/\partial T$, ΔT is the temperature difference across the tank, K is the permeability of the porous medium, ν is the kinematic viscosity, and $\kappa^* = k_m/(\rho c)_f$, the ratio of the heat conductivity of the medium to the heat capacity of the fluid.

The linear stability problem of a horizontal porous layer saturated with a stabilizing salinity gradient and heated from below was considered by Nield (1968). For the boundary conditions that the top and bottom walls are rigid with given temperature and salinity, Nield found that the onset of the instability is in the oscillatory mode and that the critical thermal Rayleigh number $R_{T,c}$ is related to the solute Rayleigh number

$$R_S = \frac{g\beta \Delta S K d}{\nu \kappa_S'},$$

with $\beta = \rho^{-1}\partial\rho/\partial S$, ΔS the solute concentration difference across the layer, and κ_S' the solute diffusivity in the porous medium. Rubin (1973) has extended Nield's analysis to nonlinear salinity profiles with given values of salinity maintained at the top and bottom walls. It was assumed that the changes in the nonlinear profile due to salt diffusion took place slowly so that a quasi-steady stability analysis could be made. For a cosine profile and R_S up to 800, the results show that there is a stabilizing effect for the onset of monotonic instability. But there is almost no effect for the onset of the overstability mode. We note here that the critical thermal Rayleigh number for the onset of the overstability mode is much smaller than that for the monotonic

mode. Taunton, Lightfoot & Green (1972) have considered the salt-finger convection case in a porous layer.

The only experimental work in double-diffusive convection in porous media has been carried out by Griffith (1981). He obtained values of heat and salt fluxes through an interface between two layers of fluid with different temperatures and salt concentrations. This was applied to the Wairakei geothermal system, and the observed values were consistent with those found in laboratory experiments.

The present experiments consider the onset of double-diffusive convection in a finite box of porous medium. The rigid top and bottom walls of the box provide a linear basic-state temperature profile but allow only a nonlinear time-dependent basic-state salinity profile. Although this configuration differs from the onset problem treated by linear theory in the literature (Nield 1968; Taunton *et al.* 1972), it is equally relevant to problems of practical interest.

In the following, we first describe the experimental apparatus and procedure. The results with a uniform-concentration fluid and the results with a salinity gradient are discussed next. Since the critical ΔT ranges from 10 °C to 40 °C, the properties of the fluid, and thus those of the medium, vary across the layer. All experimental parameters are calculated at the mean temperature of the layer, which was kept at approximately the same value for most of the tests. Finally, some results from linear stability theory are presented, where the theory has been extended to account for the effects of temperature-dependent viscosity and volumetric expansion coefficients and the nonlinear basic-state salinity profile.

2. Experimental apparatus and procedure

The experiments were performed in a box with inside dimensions of 24 cm × 12 cm and 4 cm high. The sidewalls of the box were made of glass, and the top and bottom constant-temperature walls were made of brass. The top wall, which was removable, was provided with passages through which water from a constant-temperature bath could circulate. The bottom wall was of a sandwich construction, consisting of a bottom plate made of aluminium in which water passages were provided, and a top plate made of brass. Sandwiched in between these two plates was on RdF Microfoil heat flux sensor with dimensions 4 cm × 1.5 cm and 0.15 cm thick. The sensor was located at the centre of the aluminium plate, from which sufficient material was removed to accommodate the sensor. In order to ensure good thermal contact between the aluminium plate, the heat flux sensor, and the brass plate, a Dow Corning silicone heatsink compound was applied to all contact surfaces. Thermocouples were embedded in the top and bottom walls near the inside surfaces at the centre and at the periphery of each wall. The box was insulated on all sides with 5 cm thick styrofoam. Water at different constant temperatures was supplied by two separate constant-temperature baths. A sketch of the apparatus is shown in figure 1. The heat flux sensor was calibrated by filling the box with glycerine and imposing a stable temperature difference across the box. The heat flux was calculated from the temperature difference using the heat conductivity values given by Segur (1953).

The solid matrix consisted of glass beads with a nominal diameter of 0.3 cm. The permeability K of the water-saturated porous medium was obtained by measuring the pressure drop through a column 55 cm in height and 8.15 cm in diameter. From the data presented in figure 2, in which the volumetric flow rate is shown as a function of pressure loss in centimetres of water, the value of K was determined to be 0.85×10^{-4} cm^2. This value is slightly higher than the value of 0.79×10^{-4} cm^2

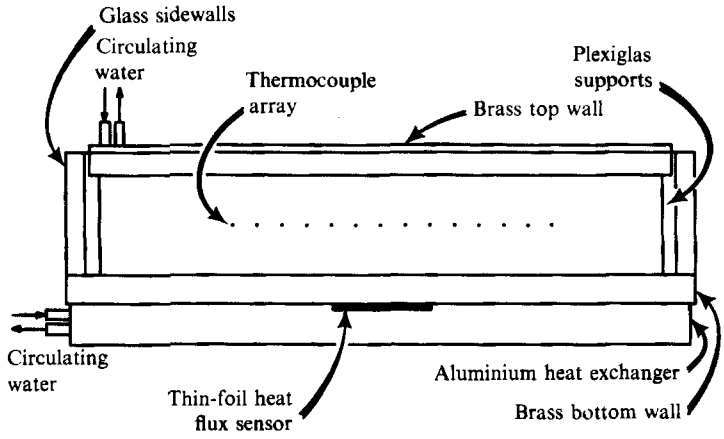

FIGURE 1. Experimental apparatus.

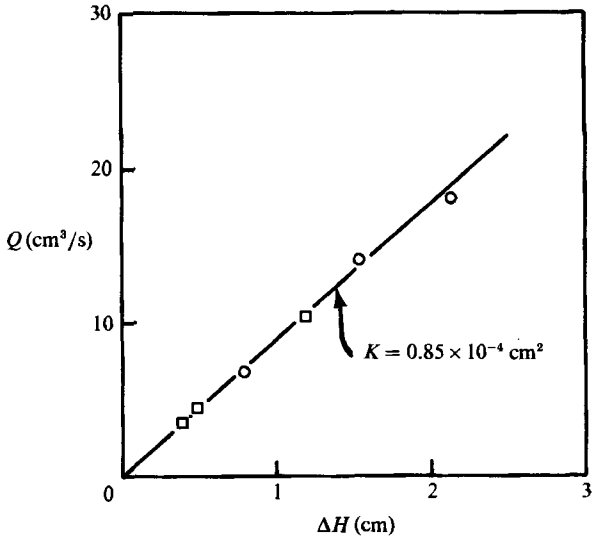

FIGURE 2. Pressure drop characteristics through a 55 cm high column of porous medium.

obtained by using the well-known Kozeny–Carmen relationship (Combarnous & Bories 1975):

$$K = \frac{d_1^2}{172.8}\frac{\epsilon^3}{(1-\epsilon)^2}, \tag{2}$$

where d_1 (the bead diameter) = 0.3 cm and $\epsilon = 0.385$, the measured value of porosity.

Since it is difficult to visualize the motion of the fluid within the medium, temperature distributions in the porous medium were used to infer the pattern of convective motion. It would, therefore, provide an independent check on the critical ΔT for the onset of convection. Temperatures at selected locations at the mid-height of the layer were measured by thermocouples which were fixed onto a grid. The grid was made of a Plexiglas frame spanning the inside of the box, with two tightly stretched nylon lines, one in the longitudinal (x) direction and the other in the lateral (y) direction. Thermocouples made of 36 gauge copper and constantan wires were

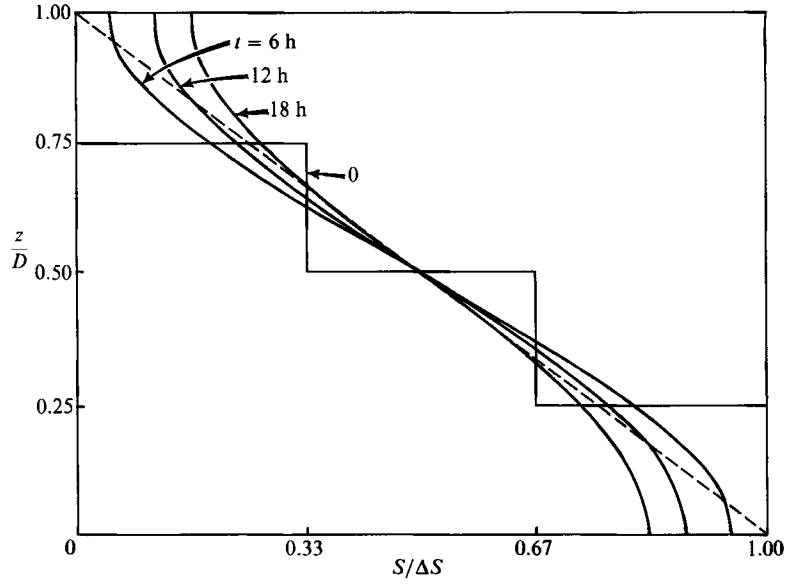

FIGURE 3. Calculated vertical salinity distribution in the box at time = 0, 6, 12, and 18 h after filling.

glued onto the nylon lines, 1 cm apart in the longitudinal direction and 1.4 cm apart in the lateral direction. Not counting the thermocouple in the centre, there were 13 thermocouples in the x-direction covering a distance of 13 cm, and 6 thermocouples in the y-direction covering a distance of 9 cm. The temperatures were recorded by an automated data-logging system using an Apple II computer as the controller and a Fluke multimeter.

For experiments with water, the box was first filled with the glass beads and distilled water to the 2 cm level. In the filling process, care was taken to eliminate all air bubbles. The thermocouple grid was laid on top of the 2 cm layer with the frame resting on Plexiglas stays, 2 cm in height, fixed at the two ends of the box. The filling was continued until a height of 4 cm was reached. The constant-temperature wall was then carefully put on top of the porous layer with two ends resting on the frame of the thermocouple grid, which was also 2 cm in height. Care was taken not to trap any air bubbles between the porous layer and the wall.

For experiments with a salinity gradient, the box was filled in four layers, each 1 cm thick. Glass beads were first mixed with salt solutions of different concentrations in separate beakers. The beads and the salt solution were transferred into the box carefully to fill the successive 1 cm layers. After filling the box, the discrete salt layers were allowed to diffuse approximately for 12 h to achieve a smooth gradient before starting the experiment. We have made a one-dimensional diffusion calculation for the vertical salt concentration distribution in the box. The results are shown in figure 3. It is seen that at 6 h, the gradient was already very smooth, and it was decreasing slowly. By 18 h, the gradient at the mid-height of the box became very close to the intended value. It is noted that in most experiments, the onset of convection generally happened around 18 h after filling. Even though at this time the salinity gradient at the middle of the layer approached the intended value, the salt distribution near the top and bottom walls was far from linear, as assumed in the theoretical considerations.

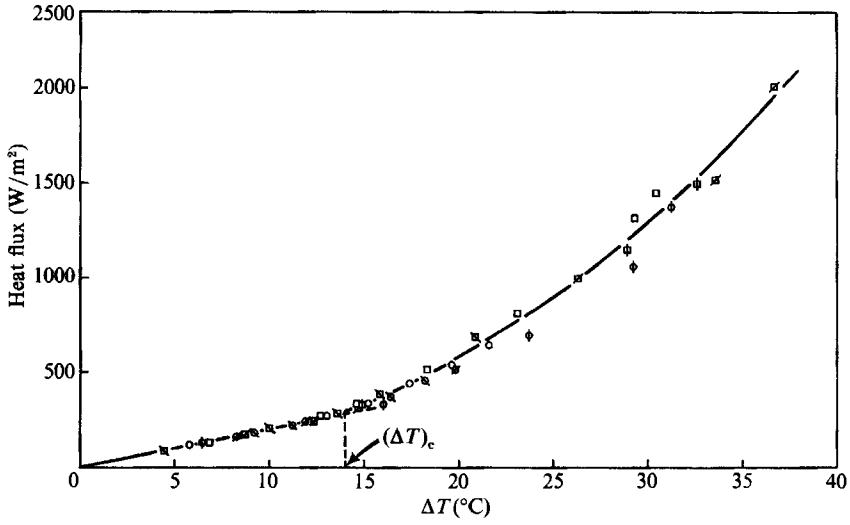

FIGURE 4. Heat flux curve for water (circles) and 0.3% salt solutions (squares).

To start each experiment, the temperature of the bottom wall was increased by a preset amount, while the temperature of the top wall was decreased by the same amount, thus keeping the mean temperature constant. After each adjustment of the ΔT, the temperature in the porous medium and the heat flux became steady, generally in less than 1 h, except at the critical ΔT for the salinity gradient case. The thermal diffusion time based on a layer thickness of 2 cm is 2000 s. To be sure that equilibrium conditions were obtained at each temperature setting, the ΔT was adjusted every 2 h. In this manner, the ΔT was increased to the critical value and beyond. For the uniform fluid, the onset of convection was identified by the change in the slope of the heat flux versus ΔT curve and the temperature distribution in the layer. For the double-diffusive case, this procedure was modified because of the dramatic increase of heat flux at the onset of convection. It usually takes up to three or four experiments to precisely determine the onset point.

3. Experimental results

3.1. *Fluid with uniform concentration*

To test the experimental system and to gain some insight into the convection process in a porous medium saturated with fluids of uniform concentration, we conducted a number of experiments with water and with a salt solution of 0.3% concentration. The results are presented in terms of heat flux curves and temperature distributions. The tests were carried out with $T_m \approx 22$ °C. The variation of heat flux with the ΔT imposed across the box is shown in figure 4. It is seen that in the conduction regime, $\Delta T < 14$ °C, the heat flux is a linear function of ΔT, and the slope is the heat conductivity of the porous medium k_m. The value of k_m thus obtained, 0.8 W/m °C, is within 5% of the recommended theoretical value, which is calculated by

$$k_m = (1-\epsilon)\, k_g + \epsilon k_f, \tag{3}$$

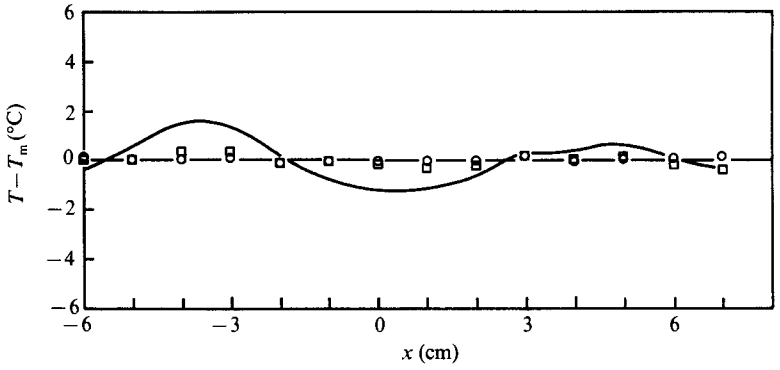

FIGURE 5. Longitudinal temperature distribution: ○, $\Delta T = 8.0$ °C; □, 13.8 °C; —, 15.0 °C.

in which k_g and k_f are the thermal conductivities of the glass and the fluid, respectively. When the temperature difference exceeds 14 °C, the heat flux departs from the linear relationship, indicating the presence of convection.

The critical ΔT of 14 °C was corroborated by the change in the character of the longitudinal temperature distribution at values of ΔT lower and higher than 14 °C. In figure 5, we present the longitudinal temperature distribution at $\Delta T = 8.0$ °C, 13.8 °C, and 15.0 °C. These data were obtained from two different test cases with slightly different mean temperatures. To eliminate any possible confusion, the temperature data are shown as the difference from the mean values. It is seen that up to $\Delta T = 13.8$ °C, the temperature in the longitudinal direction was essentially constant. At $\Delta T = 15$ °C, however, the temperature distribution became wavy, indicating the presence of convection.

Based on the properties of the fluid and of the porous medium evaluated at the mean temperature at the time of onset of convection, with $\Delta T_c = 14$ °C, the critical Rayleigh number, $R_{T,c}$, was found to be 56, which is 40% higher than the value of $4\pi^2$ (Lapwood 1948). The same data points presented in figure 4 were converted to points in the Nusselt number–Rayleigh number plot, as shown in figure 6. As can be seen, $R_{T,c} = 56$ is a good estimate of the point of onset of convection.

In the late 1960s and early 1970s, four sets of authors (Elder 1967; Katto & Masuoka 1967; Combarnous & LeFur 1969; and Buretta 1972) experimentally confirmed the value of $4\pi^2$. Elder's experiments were carried out in a large circular tank whose diameter could be adjusted to 180 cm. The bottom heated region was confined to a central circular area whose diameter was smaller than that of the tank, but much larger than the thickness of the porous layer. Glass spheres of diameters ranging from 0.3 to 1.8 cm were used as the solid matrix. There was no mention of the type of fluid used to saturate the solid matrix, nor were any property values given. His results, in the form of Nusselt number Nu plotted against Rayleigh number, yield a critical Rayleigh number of 40 ± 10%.

Katto & Masuoka (1967) conducted their experiments in a circular geometry with a diameter of 10 cm. The thickness of the layer was variable, with 0.9 cm as the standard. Small spheres of glass, steel, and aluminium were used as the solid matrix, and nitrogen was the saturating fluid. The data were presented over a range of d_1/d, the ratio of the diameter of the spheres to the thickness of the layer, $0.05 \leqslant d_1/d \leqslant 1$. The critical Rayleigh number of $4\pi^2$ gives a straight line which goes

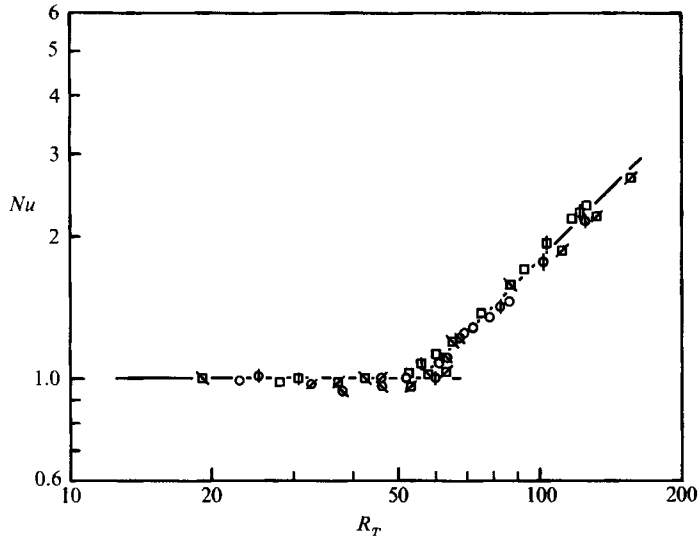

FIGURE 6. Nu versus R_T for fluids with uniform concentration. Circles are for water; squares are for 0.3% salt solution.

through most of the data points in a log–log plot. But for the five data points obtained with glass spheres with $d_1/d < 0.1$, all experimental values were below $4\pi^2$, with two of the points at $R_{T,c} = 21.6$ and 26, which were 46% and 35%, respectively, below the theoretical value.

Combarnous & LeFur (1969) carried out their experiments in a rectangular box somewhat larger than ours, 60 cm × 37 cm and 5.35 cm high. The solid matrix consisted of small beads made of glass, polypropylene, lead, and quartz (sand), with diameters ranging from 0.09 to 0.4 cm. The fluid was either water or oil. The only property reported was the porosity ϵ. The results were presented in the form of an Nu versus R_T plot, and the critical value was determined to be within 10% of $4\pi^2$.

The experiments carried out by Buretta (1972) were conducted in a circular tank with a diameter of 29.2 cm. The height of the tank was adjustable, varying from 4.28 to 8.81 cm. The solid matrix consisted of glass beads with diameters of 0.3, 0.6 and 1.43 cm. The critical Rayleigh number obtained for 0.3 cm beads was 39.28, with an estimated error of 5%. Upon closer examination, the values of permeability K and the medium thermal conductivity k_m used by Buretta were significantly different from those used by us: $K = 0.761 \times 10^{-4}$ cm^2, $k_m = 0.94$ W/m °C; and $K = 0.85 \times 10^{-4}$ cm^2, $k_m = 0.83$ W/m °C respectively. To obtain K, Buretta used the Kozeny relation with a correction factor to account for wall effects. The thermal conductivity of the porous layer k_m was determined by experiment both in Buretta's work and ours. The thermal conductivity of the glass may be calculated from the value k_m Buretta obtained $k_g = 1.16$ W/m °C, and we obtained $k_g = 0.7$ W/m °C. The former corresponds to a borosilicate glass, and the latter to a soda-lime glass.

The effect of finite geometry has been considered by Beck (1972) using a linear stability analysis. His results show that unless the horizontal dimensions of the box are smaller than the vertical dimensions, the finite geometry has negligible effect on $R_{T,c}$.

Since the temperatures can be determined to ±0.1 °C, the major contributing errors to $R_{T,c}$ are the errors in the permeability, K, and the heat conductivity of the

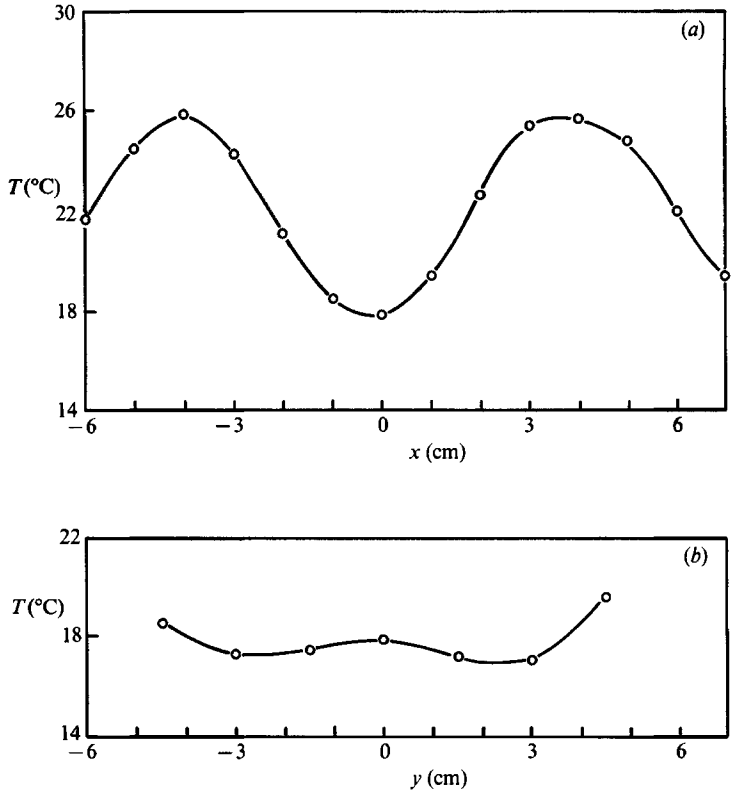

FIGURE 7. (*a*) Longitudinal and (*b*) lateral temperature distributions in a water-saturated porous layer at $\Delta T = 17.4$ °C, $R_T = 69.6$.

medium, k_m, both measured quantities. Our estimates of the errors in measurement are $\pm 10\%$ for K and $\pm 5\%$ for k_m. Together with the possible errors in the property values because of the uncertainties in the temperature, the Rayleigh number that we evaluated may be in error by $\pm 20\%$. It must be pointed out that the K-value measured in a cylinder 55 cm in height may not be the same as that for a horizontal layer 4 cm in thickness. Furthermore, since $K \propto \epsilon^3$, if the porosity of the porous layer in the test tank is 15% lower than that in the test cylinder for pressure drop measurements, the resulting $R_{T,c}$ would be very close to $4\pi^2$.

The temperature distribution in the middle of the porous layer in the longitudinal and lateral directions at a supercritical Rayleigh number of 69.6 are shown in figure 7. The longitudinal temperature distribution indicates that there was a cold descending plume in the middle and two hot rising plumes each at 4 cm from the middle. The temperatures in the lateral direction, except the one at 4.5 cm, were sensibly constant. A convection pattern consisting of rolls parallel to the short side of the box would give a temperature distribution such as the one presented in figure 7. This is confirmed by the flow visualization photograph shown in figure 8.

The flow visualization was obtained by removing the top wall and placing the rheoscopic concentrate uniformly on the top surface of the porous layer. At the descending plumes, the particles were transported into the porous layer, thus leaving dark areas. These particles would later surface at the locations of the hot rising plumes, resulting in white areas. The dark and white areas in the photo indicate the

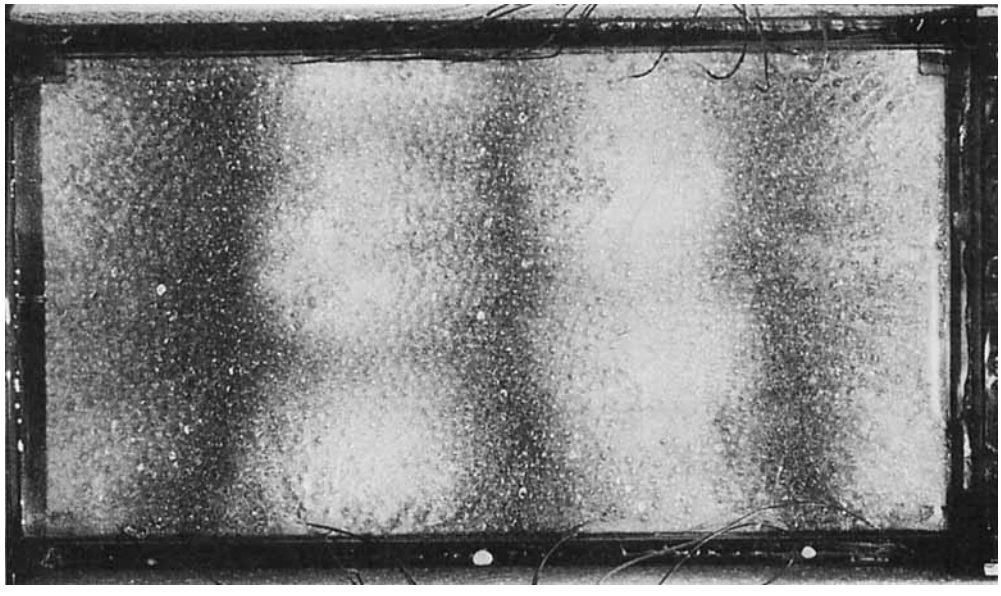

FIGURE 8. Convection pattern of the water-saturated porous layer.

presence of three pairs of counter-rotating convection rolls. The sense of circulation is that of two rising plumes at the two ends of the box.

The results obtained with the 0.3 % salt solution were essentially the same as those obtained with water. We conducted these tests to reassure ourselves that the possible effects due to thermal diffusion, or the Soret effect, were negligible at such low salt concentrations and the short timescale of our experiments (see, for example, McDougall 1983).

3.2. *Double-diffusive results*

When the porous layer was saturated with a salinity gradient, the result was dramatically different, as evidenced by the heat flux curve shown in figure 9. This experiment was carried out with an initial salinity gradient of 0.15 % cm^{-1}. The critical ΔT was found to be 35.1 °C, more than twice that for the uniform-concentration fluid. At this critical ΔT, the heat flux increased slowly from 730 W/m^2 to its final steady value of 1670 W/m^2 in 3 h. At the same time, the ΔT across the box slowly decreased because of the efficient transport of heat by convection, even though the two baths were kept at their respective preset temperatures. After the heat flux had reached the steady value, there was continuous adjustment of the convection pattern so that temperature distributions within the layer did not reach their final steady state until 5 h after the onset of convection.

As the ΔT ws further increased to 38 °C, the heat flux curve became nonlinear and had a much larger slope than in the conduction case. When the ΔT was slowly reduced, the heat flux curve approached the conduction line, smoothly joining the latter at approximately 14 °C. This hysteresis phenomenon can be explained as follows. Because of the stable salinity gradient, the onset of convection is delayed to a higher temperature difference. Once convection sets in, the stabilizing gradient is gradually destroyed. When the mixing is complete, the fluid behaves as one with a uniform concentration. It is recalled that the experiments conducted by Hurle &

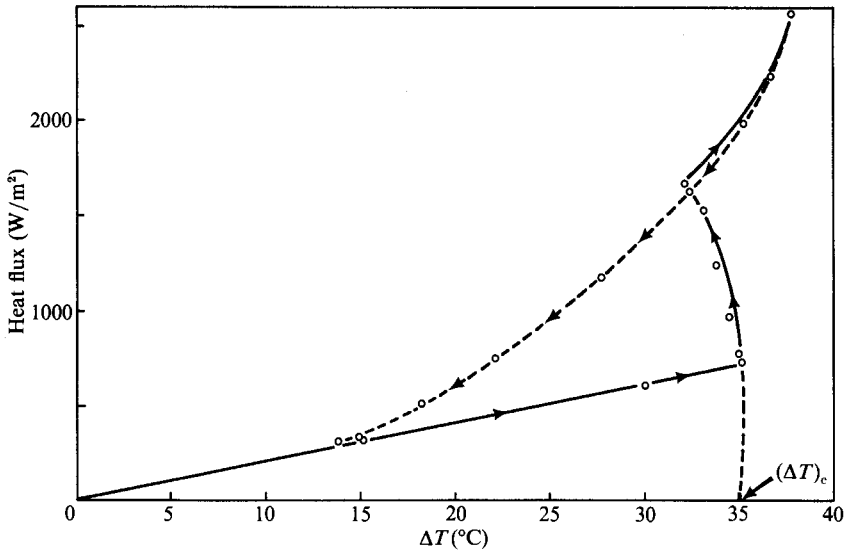

FIGURE 9. Heat flux curve for a porous layer saturated with a salt solution gradient of 0.15% cm^{-1}, showing hysteresis effect.

Jakeman (1971), Caldwell (1974), and Platten & Legros (1984) show that thermal diffusion effects would also cause hysteresis loops in the heat flux curves. But the present phenomenon is due to the overturning of the imposed initial salinity gradient rather than the one resulting from thermal diffusion effects.

The temperature distributions in the longitudinal and lateral directions 3 h after the onset of convection when $\Delta T = 32.1$ °C are shown in figure 10. Now the temperature variations in the lateral direction become comparable with those in the longitudinal direction, indicating the presence of three-dimensional convection. This was confirmed by the flow visualization photograph, shown in figure 11, taken during a test with a salinity gradient of 0.225% cm^{-1} at a comparable time in the experiment. The photograph indicates that there were two large convection cells in the central portion of the tank and six smaller ones along the periphery. The three-dimensional convection pattern may be due to the fact that the convection is in a highly supercritical state for a uniform-concentration fluid.

The slow approach to the uniform-concentration case is evidenced by the temperature distribution obtained 5 h and 14 h after the onset of convection, as shown in figure 12. The circles denote the data obtained 5 h after the onset of convection when the heat flux was at 1670 W/m^2 and $\Delta T = 32.1$ °C. It is seen that the temperature variation in the lateral direction had decreased to less than 5 °C, and the temperature variation in the longitudinal direction became more sinusoidal. The data taken 14 h after the onset of convection when ΔT was 18.2 °C (denoted by the squares) show a further decrease in the lateral temperature variation to less than 2.5 °C and a slight readjustment in the convection cell size. Comparing with the data for the case with water (figure 7), the longitudinal temperature variation was about 3 °C less for the present case, which could be caused by some residue effects of the initial salt stratification.

Another set of experiments was carried out with a salinity gradient of 0.225% cm^{-1}. The heat flux curve obtained from one of the tests is shown in figure 13, together with all the previous cases considered. To avoid confusion, only data points

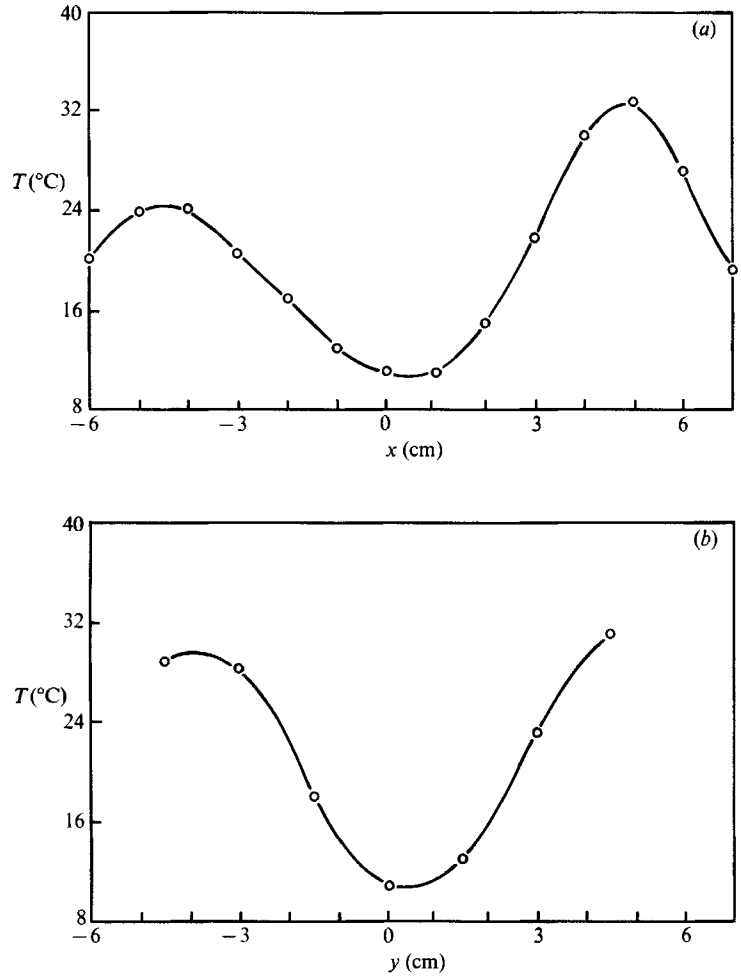

FIGURE 10. (*a*) Longitudinal and (*b*) lateral temperature distributions in a porous layer saturated with a salt solution gradient of 0.15% cm^{-1} 3 h after the onset of convection at $\Delta T = 32.1$ °C.

from the two salinity gradient cases are presented. In the conduction phase, data from all test cases, with or without salinity gradients, lie along the same straight line, indicating that the value k_m is constant. The dashed line is the heat flux curve during the convection phase for the uniform-concentration fluid.

Linear stability theory predicts that the onset of convection is in the oscillatory mode. We have attempted to record such oscillations. Figure 14 shows a representative thermocouple output versus time after the reading first started to deviate from the steady conduction value for a typical 0.15%/cm experiment. The thermocouple was located in the centre of the tank at the mid-height of the layer. The time period for the first complete oscillation exhibited is about 28 min. However, as the figure shows, regular oscillations are not sustained. There is a larger monotonic decrease in the temperature after the first oscillation, before a second oscillation cycle of the same period occurs. Figure 15 shows similar behaviour in a 0.225%/cm experiment. In this case, the output from the differential thermocouple probe versus time is shown as it begins to vary from the steady conduction value. The first

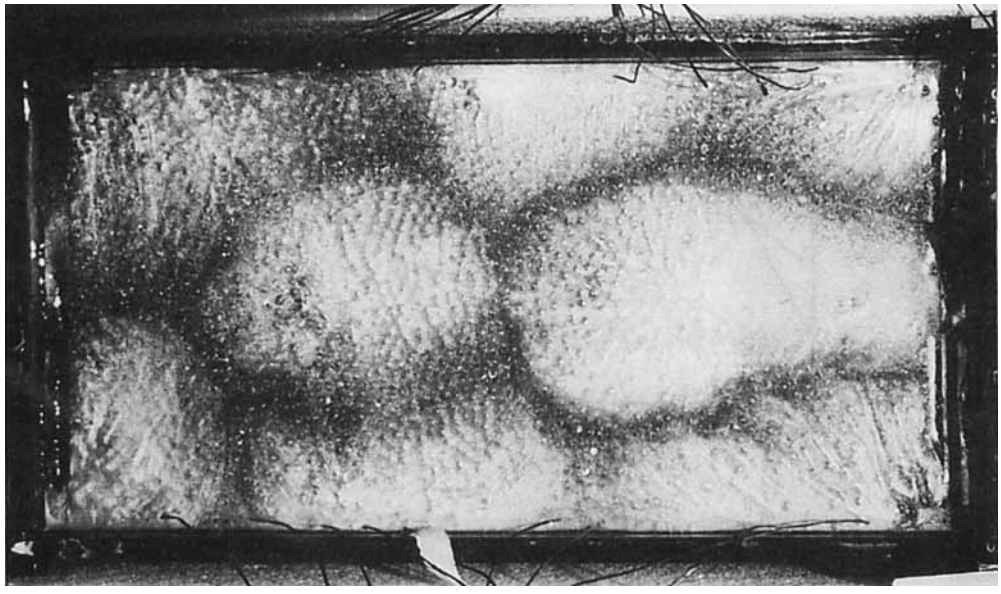

FIGURE 11. Convection pattern in a porous layer saturated with a 0.225 % cm^{-1} salinity gradient.

discernible complete oscillation starting from $t = 0$ has a period of approximately 22 min. Just as in the 0.15%/cm case, the oscillations do not persist, but instead a significant irregular variation in temperature occurs.

4. Discussion

The experimental results are summarized in table 1. Values for the thermal and solute Rayleigh numbers and the oscillation frequencies ω for the experiments were calculated using the following values for the properties, which were independent of temperature: $\kappa^* = 2.0 \times 10^{-3}$ cm^2/s, $\kappa'_S = 4.0 \times 10^{-6}$ cm^2/s (Wooding 1959), and $\beta = 0.7 \times 10^{-2}\,\%^{-1}$. Values of kinematic viscosity and thermal expansion coefficients were evaluated at the mean temperature values listed in table 1. The measured value of the permeability was used. The diffusivity ratio τ, based on the effective diffusivities, is 0.002 for the experiments here.

One objective of the experimental investigation it to test the predictions of linear theory for onset of the instability. In order to make the comparison meaningful, it is necessary to modify the existing theory to account for the nonlinear salinity basic state and property variation with temperature.

The rigid walls in the experimental facility prevented the maintenance of a constant salt concentration difference across the layer. The non-diffusive boundaries yield a nonlinear time-dependent salinity basic-state profile. However, owing to the very small diffusivity of NaCl ($\tau = 0.002$), for the purpose of determining the onset criterion from linear theory, it is reasonable to assume that the profile is quasi-steady. An approximation of the salinity profile that exists close to onset in the experiments is used in the quasi-steady linear analysis.

The temperature differences across the layer at onset for the double-diffusive experiments are 35 °C and 41 °C. These temperature differences are large enough to

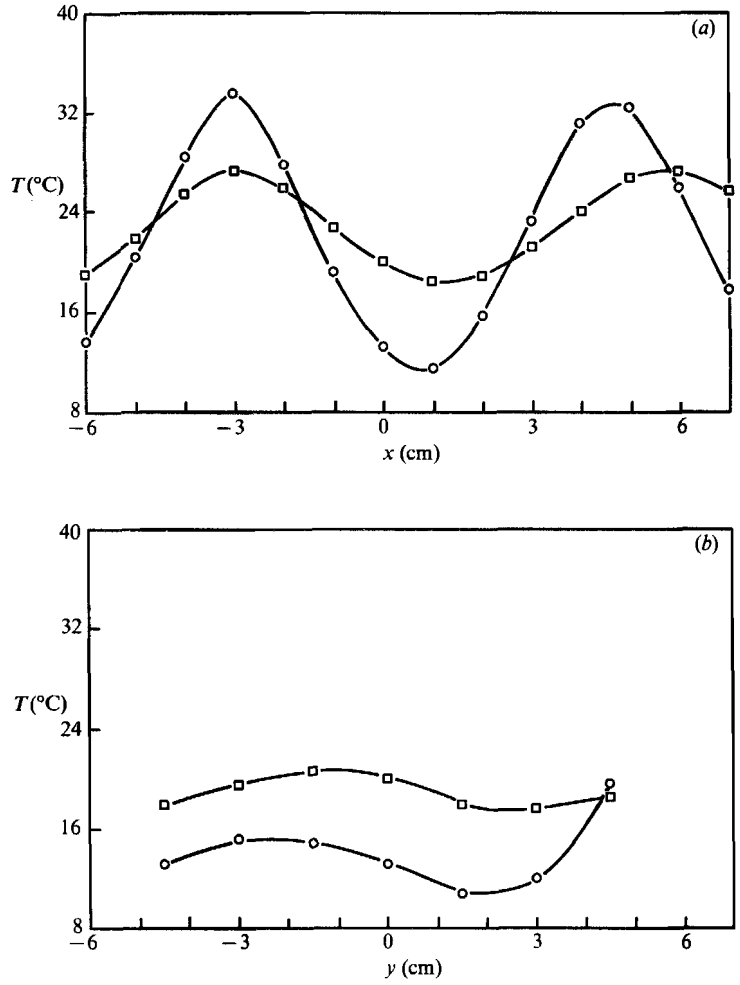

FIGURE 12. (a) Longitudinal and (b) lateral temperature distributions in a porous layer saturated with a salt solution gradient of 0.15% cm^{-1}: ○, $\Delta T = 32.1$, $t = 5$ h; □, $\Delta T = 18.2$, $t = 14$ h.

warrant evaluation of the effect of temperature-dependent thermal expansion coefficient and viscosity for water on the linear theory results. An outline of the analysis used to obtain the linear theory predictions discussed in this section is given in the Appendix.

Table 2 is a summary of the critical conditions from linear theory for the two experimental values of solute Rayleigh numbers. Theoretical values for the critical thermal Rayleigh number, the oscillation frequency, and the dimensional wavelength are given for the following three sets of model assumptions: (1) constant properties and a linear solute basic state assuming fixed solute values at the boundaries (the original problem considered by Nield 1968); (2) linear solute basic state but with temperature-dependent thermal expansion coefficient α and viscosity μ; and (3) quasi-steady representation of the experimental solute basic state including the temperature variation of the two properties. It is seen that with variable α and μ, both the critical Rayleigh number and the critical wavelength are reduced. When the cosine profile is assumed for the salinity distribution, the critical Rayleigh numbers

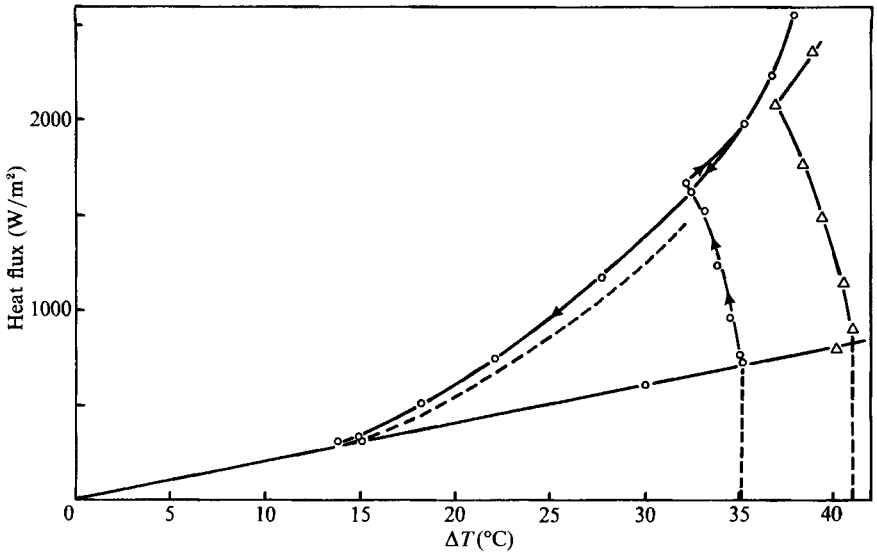

FIGURE 13. Heating curves for all cases considered: ○, 0.15% salinity gradient; △, 0.225% salinity gradient; ----, uniform concentration.

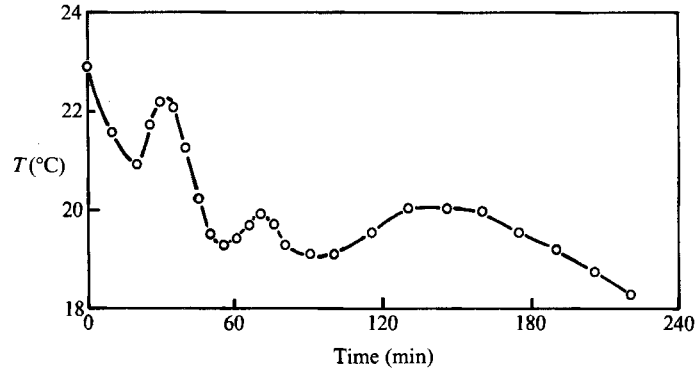

FIGURE 14. Temperature at a point in the porous layer monitored as a function of time from the onset of convection for a 0.15%/cm salinity gradient.

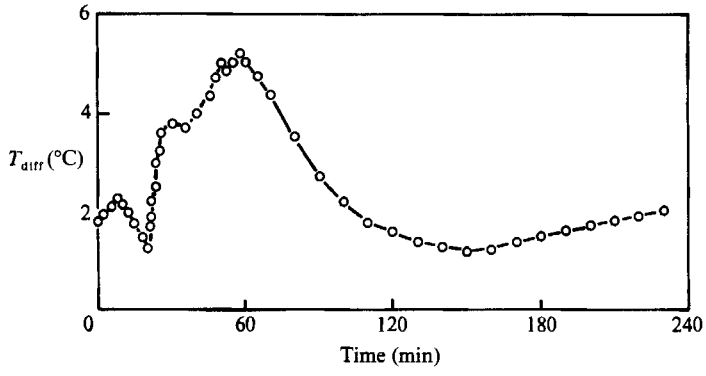

FIGURE 15. Output from a differential thermocouple monitored over time for a 0.225%/cm salinity gradient.

Salinity gradient	No. of tests	T_m (°C)	ΔT (°C)	R_S	$R_{T,c}$	ω (s^{-1})
0	8	22	13.8	0	55	—
0.15%/cm	8	23	35	37800	150	0.0037
0.225%/cm	5	25	41	59100	200	0.0048

TABLE 1. Summary of experimental results

	$R_S = 37800$			$R_S = 59000$		
Property variation	R_T	ω (s^{-1})	λ (cm)	R_T	ω (s^{-1})	λ (cm)
Constant	180	0.0065	8.0	259	0.0081	8.0
Variable α and μ	162	0.0089	6.2	222	0.0135	5.3
Nonlinear S-profile, variable α and μ	145	0.0082	5.8	192	0.013	4.7

TABLE 2. The effect of a nonlinear salinity basic state and temperature-dependent thermal expansion coefficient and viscosity on the linear theory onset criteria

	Measured K			Reduced K	
R_S	Theory	Exp.	R_S	Theory	Exp.
0	39.5	55	0	39.5	39.5
37800	145	150	29100	119	109
59100	192	200	45500	157	146

TABLE 3. Comparison of onset criteria calculated using measured versus reduced permeability values

for the two different salt gradient cases are within 10% of our experimental results.

We also made a set of calculations using a reduced value of permeability K so that our experiments with a zero salinity gradient would yield a critical Rayleigh number of $4\pi^2$. The solute Rayleigh numbers corresponding to the two experimental cases reduced to 29100 and 45500, respectively. The critical thermal Rayleigh numbers obtained by theory and experiment are shown in table 3, together with the corresponding values using the measured value of K. It is seen that with the reduced K, the experimental values are reduced to 109 and 146, while the linear stability theory predicts 119 and 156, still within a 10% relative error. These results show that our experiments with or without the salinity gradient are self-consistent.

5. Conclusions

(*a*) For a horizontal layer of porous medium saturated with a fluid having a stabilizing salinity gradient, the heat flux is found to increase dramatically from the conduction value at the critical temperature difference.

(*b*) The dramatic behaviour exhibited at onset overshadows the oscillatory double-diffusive mechanism associated with infinitesimal motion in a porous layer having a stabilizing concentration gradient and heated from below.

(*c*) The heat flux exhibits hysteresis effects as the ΔT is first increased beyond the critical value and then decreased below the critical value and back to the level that yields a conduction solution.

(*d*) The developed flow pattern in the double-diffusive experiments is found to consist of three-dimensional cells, while two-dimensional rolls are observed for single-component convection in the same apparatus.

(*e*) Agreement to within 10% for the critical thermal Rayleigh number is obtained between the experiments and linear theory if the conditions of the experiments, namely, the nonlinear salinity basic state and temperature-dependent thermal expansion coefficient and viscosity, are properly accounted for in the theory.

The financial support provided by the National Science Foundation through grant MEA-82-06087 is gratefully acknowledged. An earlier version of this paper was presented as the ASME Symposium 'Double-Diffusive Motion' in 1985.

Appendix. Linear stability theory

This appendix briefly describes the analysis used to determine the effect of a nonlinear salinity basic state and temperature-dependent viscosity and thermal expansion coefficient on the oscillatory onset predictions from linear stability theory. The analysis is an extension of the problem first considered by Nield (1968).

The starting point of the analysis is the set of model equations expressing conservation of mass, momentum, energy, and species concentration for a porous medium saturated with an incompressible fluid. For the buoyancy-driven problem, the Boussinesq approximation is employed, but generalized to include temperature-dependent properties.

Thermal expansion coefficient variation is included by assuming the density to be quadratic in temperature as follows:

$$\rho = \rho_0[1-\alpha(T-T_0)-\alpha_2(T-T_0)^2+\beta(S-S_0)], \tag{A 1}$$

in which α and α_2 are the first and second thermal expansion coefficients and the subscript zero denotes the reference state. The viscosity of the fluid is assumed to be

$$\mu = \mu_0 F(T-T_0), \tag{A 2}$$

in which F is the empirical curve fit given by Weast (1977).

For a porous medium saturated with such an incompressible fluid, the governing equations are

$$\boldsymbol{\nabla}\cdot\boldsymbol{u} = 0, \tag{A 3}$$

$$\frac{\rho_0}{\epsilon}\frac{\partial \boldsymbol{u}}{\partial t} = -\boldsymbol{\nabla}p+\frac{\mu_0}{K}F(T-T_0)\,\boldsymbol{u}+\rho_0\boldsymbol{g}[1-\alpha(T-T_0)-\alpha_2(T-T_0)^2+\beta(S-S_0)], \tag{A 4}$$

$$\frac{1}{M}\frac{\partial T}{\partial t}+\boldsymbol{u}\cdot\boldsymbol{\nabla}T = \kappa^*\nabla^2 T, \tag{A 5}$$

$$\epsilon\frac{\partial S}{\partial t}+\boldsymbol{u}\cdot\boldsymbol{\nabla}S = \kappa_S'\nabla^2 S, \tag{A 6}$$

in which $\boldsymbol{u}$ is the filtration velocity vector, $\boldsymbol{g}$ is the gravitational acceleration vector. M is the ratio of heat capacities

$$M = \frac{(\rho_0 c)_f}{(\rho_0 c)_m}.$$

where c is the heat capacity and the subscripts f and m denote fluid and porous medium, respectively. κ'_S is the diffusivity of salt in a porous medium, which is usually less than that in a fluid (Wooding 1959). Equation (A 4) is the Darcy's equation with the unsteady inertial term retained. Equations (A 5) and (A 6) differ slightly from those given by Nield (1968) by the presence of M in the energy equation and ϵ in the solute conservation equation. A more careful balance of heat and solute flux through a differential control volume would yield the extra factors M and ϵ in their respective equations (Combarnous & Bories 1975).

The domain is a porous layer confined between two infinite horizontal rigid plates set at a distance d part. Let the rectangular coordinates (x, y, z) be such that z is vertically upwards, perpendicular to the plates. The two plates are kept at different but constant temperatures, which yields a linear temperature basic-state profile in the quiescent fluid-saturated porous medium.

A representation of the nonlinear salinity basic state that exists close to onset in the experiments is used in a quasi-steady analysis. Figure 3 shows the diffusion of the salinity basic state with time. After preliminary testing in the experiments, it was possible to reach the required onset temperature difference at approximately the same time after the salinity gradient was established. This time was, on average, 18 h. The salinity profile at this time is shown in figure 3. For quasi-steady stability analysis, a good representation of the salinity basic state is given by

$$S_B(z) = S_0 + \chi \frac{\Delta S}{2} \cos\frac{\pi z}{d}, \tag{A 7}$$

where S_0 is the reference salinity at the mid-height of the layer, ΔS is the initial difference in the salinity values between the top and bottom of the layer, and χ is the fractional amount of ΔS that exists at onset ($\chi = 0.66$ at 18 h in the experiments).

Let w denote the vertical component of the perturbation velocity, θ the perturbation temperature, and γ the perturbation solute concentration. By the usual procedure in eliminating the pressure, we obtain the following set of linearized equations:

$$\frac{1}{\epsilon}\frac{\partial}{\partial t}\nabla^2 w = g\left\{\alpha\left[1+\alpha'\left(1-\frac{2z}{d}\right)\right]\nabla_1^2\theta - \beta\nabla_1^2\gamma\right\} - \frac{\nu_0}{K}\left[F(\bar{T})\nabla^2 w - B\frac{\mathrm{d}F(\bar{T})}{\mathrm{d}T}\frac{\partial w}{\partial z}\right], \tag{A 8}$$

$$\frac{1}{M}\frac{\partial\theta}{\partial t} = Bw + \kappa^*\nabla^2\theta, \tag{A 9}$$

$$\epsilon\frac{\partial\gamma}{\partial t} = \tfrac{1}{2}\pi\chi B_S \sin(\pi z/d)\, w + \kappa'_S\nabla^2\gamma, \tag{A 10}$$

where $\alpha' = \alpha_2/\alpha$, ∇_1 is the horizontal Laplacian, $\nu_0 = \mu_0/\rho_0$, $\bar{T} = T_B - T_0$, $B = \Delta T/d$, and $B_S = \Delta S/d$.

In order to solve the set of linear equations, solutions in the form of normal modes are assumed,

$$[w, \theta, \gamma] = [W(z), \Theta(z), \Gamma(z)]\, \mathrm{e}^{[\sigma t + \mathrm{i}(k_1 x + k_2 y)]}. \tag{A 11}$$

After the normal mode solutions are substituted into the governing equations, the following non-dimensional variables are defined:

$$\xi = \frac{\pi z}{d}, \quad \mathrm{D}^2 = \frac{\pi^2}{d^2}\frac{\mathrm{d}^2}{\mathrm{d}\xi^2},$$

$$W_1 = \frac{\pi K}{d\nu_0} W, \quad \Theta_1 = \frac{\pi^3 K \kappa^*}{d^3 \nu_0 B}\Theta, \quad \Gamma_1 = \frac{\pi^3 K k_S'}{d^3 \nu_0 B_S}\Gamma,$$

$$b^2 = \frac{d^2}{\pi^2}(k_1^2 + k_2^2), \quad \sigma_1 = \frac{d^2}{\pi^2 \nu_0}\sigma, \quad \delta = \frac{\pi^2 k}{\epsilon d^2},$$

where b is the non-dimensional wavenumber and σ_1 is the growth rate, which is assumed to be complex.

Making these substitutions, the governing set of linear PDEs (A 8), (A 9), and (A 10) reduces to the set of three second-order ODEs,

$$[F(\xi) + \delta\sigma_1]\mathrm{D}^2 - b^2)\, W_1 + \mathrm{D}F(\xi)\,\mathrm{D}W_1 = -\frac{b^2}{\pi^2} R_T \left[1 + \alpha'\left(1 - \frac{2\xi}{\pi}\right)\right]\Theta_1 + \frac{b^2}{\pi^2} R_S \Gamma_1, \tag{A 12}$$

$$\left(\mathrm{D}^2 - b^2 - \frac{Pr}{M}\sigma_1\right)\Theta_1 = -W_1, \tag{A 13}$$

$$(\mathrm{D}^2 - b^2 - \epsilon Sc\,\sigma_1)\,\Gamma_1 = -(\tfrac{1}{2}\pi\chi \sin\xi)\, W_1, \tag{A 14}$$

where the Prandtl number $Pr = \nu_0/\kappa^*$ and the Schmidt number $Sc = \nu_0/\kappa_S'$. Six boundary conditions are required. The vertical velocity is zero at the top and bottom solid boundaries and the temperature and salinity disturbances are also assumed to vanish. These conditions are specified as

$$W_1 = \Theta_1 = \Gamma_1 = 0 \quad \text{at } \xi = 0, \pi.$$

The equations (A 12)–(A 14) with the above boundary conditions yield the eigenvalue problem for the linear theory onset criterion. Because the set of equations has variable coefficients, the solution for the stability criterion must be found numerically. The Galerkin method was used to obtain the solution to the stability problem. The details of the solution procedure are given in Murray (1986).

For a porous layer heated from below subject to a stabilizing salinity gradient, the stability criterion is given by the critical values of R_T as a function of R_S, Pr, Sc, ϵ, δ, M, χ, and the assumed form of the temperature-dependent properties. Note that R_S is defined in terms of ΔS, the initial salinity difference across the layer, while χ represents the existing difference at the time of onset in the quasi-steady analysis. The solution to the stability problem also yields the oscillation frequency at onset.

REFERENCES

Beck, J. L. 1972 Convection in a box of porous material saturated with fluid. *Phys. Fluids* **15**, 1377–1383.

Buretta, R. J. 1972 Thermal convection in a fluid filled porous layer with uniform internal heat sources. Ph.D. dissertation, University of Minnesota, Minneapolis.

Caldwell, D. R. 1974 Experimental studies on the onset of thermohaline convection. *J. Fluid Mech.* **64**, 347–367.

Cheng, P. 1978 Heat transfer in geothermal systems. *Adv. Heat Transfer* **14**, 1–105

COMBARNOUS, M. A. & BORIES, S. A. 1975 Hydrothermal convection in saturated porous media. *Adv. Hydrosci.* **10**, 231–307.

COMBARNOUS, M. & LEFUR, B. 1969 Transfert de chaleur par convection naturelle dans une conche poreuse horizontale. *C. R. Acad. Sci. Paris* B **269**, 1009–1012.

ELDER, J. W. 1967 Steady free convection in a porous medium heated from below. *J. Fluid Mech.* **27**, 29–48.

GRIFFITH, R. W. 1981 Layered double-diffusive convection in porous media. *J. Fluid Mech.* **102**, 221–248.

HORTON, C. W. & ROGERS, F. T. 1945 Convection currents in a porous medium. *J. Appl. Phys.* **16**, 367–370.

HURLE, D. T. J. & JAKEMAN, E. 1971 Soret-driven thermosolutal convection. *J. Fluid Mech.* **47**, 667–687.

KASSOV, D. R. & ZEBIB, A. 1975 Variable viscosity effects on the onset of convection in porous media. *Phys. Fluids* **18**, 1649–1651.

KATTO, Y. & MASUOKA, T. 1967 Criterion for onset of convection flow in a fluid in a porous medium. *Intl J. Heat Mass Transfer* **10**, 297–309.

KOHOUT, F. A. 1965 A hypothesis concerning cyclic flow of salt water related to geothermal heating in the Floridian aquifer. *Trans. N.Y. Acad. Sci.* **28**, 249–271.

KRISHNAMURTI, R. & HOWARD, L. N. 1985 Hysteresis and transports in thermally-destabilized double-diffusive convection. *Bull. Am. Phys. Soc.* **30**, 1703.

LAPWOOD, E. R. 1948 Convection of fluid in a porous medium. *Proc. Camb. Phil. Soc.* **44**, 508–521.

MCDOUGALL, T. J. 1983 Double-diffusive convection caused by coupled molecular diffusion. *J. Fluid Mech.* **126**, 379–397.

MURRAY, B. T. 1986 Experimental and numerical investigation of double-diffusive convection in a horizontal layer of porous medium. Ph.D. dissertation, University of Arizona, Tucson.

NIELD, D. A. 1968 Onset of thermohaline convection in a porous medium. *Wat. Resources Res.* **4**, 553–560.

PLATTEN, J. K. & LEGROS, J. C. 1984 *Convection in Liquids.* Springer.

RUBIN, H. 1973 Effect of nonlinear stabilizing salinity profiles on thermal convection in a porous medium layer. *Wat. Resources Res.* **9**, 211–221.

SEGUR, J. B. 1953 Physical properties of glycerol and its solutions. In *Glycerol* (ed. C. S. Minor & N. N. Dalton), pp. 238–334. Reinhold.

TAUNTON, J. W., LIGHTFOOT, E. N. & GREEN, T. 1972 Thermohaline instability and salt fingers in a porous medium. *Phys. Fluids* **15**, 748–753.

WEAST, R. C. 1977 *Handbook of Chemistry and Physics.* Cleveland: CRC Press.

WOODING, R. A. 1959 The stability of a viscous liquid in a vertical tube containing porous material. *Proc. R. Soc. Lond.* A **252**, 120–134.